Controller Hardware-in-the-Loop Testing of a Scheduler for Microgrid Control Tasks

Siddhartha Nigam, Olaoluwapo Ajala, and Alejandro D. Domínguez-García
Department of Electrical and Computer Engineering
University of Illinois at Urbana-Champaign, Urbana, IL 61801, U.S.A
Email: {nigam4, ooajala2, aledan}@illinois.edu

***Abstract*—This paper describes the development and testing of a scheduler for coordinating pertinent control tasks in a microgrid. Our proposed microgrid control scheduler is based on a centralized framework. We provide an analytical description of the microgrid control tasks that it coordinates, and describe the operations of the scheduler. Finally, we present numerical results that demonstrate how the proposed scheduler coordinates three microgrid control tasks, namely: seamless connection of an energy resource to the microgrid, coordination of energy resources to provide frequency regulation services to the bulk grid, and intentional islanding of the microgrid.**

I. Introduction

With increasing deployment of distributed energy resources (DERs) in power distribution systems, microgrids have been posed as an effective way to manage and control such assets [1]. Microgrids have also been shown to be a promising approach for providing services to the external grid it is connected to [2]. However, to operate a microgrid reliably and effectively, in the presence of variable/intermittent demand and generation, multiple control tasks must be continuously performed. Such control tasks include frequency and voltage control, economic dispatch, ancillary services provision, seamless islanding/reconnection of the microgrid from/to the external grid, as well as seamless connection/disconnection of assets to/from the microgrid.

The main contribution of this paper is the development and testing of a mechanism for *scheduling* the execution of diverse (and possibly conflicting) control algorithms that are individually designed to perform pertinent microgrid control tasks. Such algorithms, which we developed and verified in earlier works, include schemes for: frequency control [3], voltage control [4], provision of regulation services [5], optimal asset dispatch [6], and synchronization of microgrid interconnection points [7]. Controller hardware-in-the-loop (C-HIL) testing is used to verify the effectiveness of our proposed scheduler in coordinating the execution of control tasks in the Banshee distribution network [8]—a standard microgrid test system designed for evaluation of microgrid control schemes. Our testbed setup comprises a National Instruments (NI) compact rio (cRIO) device on which we implement the different control schemes, as well as the scheduler logic. A real-time emulation of the Banshee system is developed on several Typhoon HIL hardware devices, and the cRIO is connected to assets in the network via ethernet.

Over the years, several authors have addressed the problem of managing microgrid control tasks. In [9] and [10], an energy management platform for DC/AC microgrids is proposed. The focus is on a particular control objective such as cost or loss minimization, efficient asset (energy storage) operations, and improved market strategies for revenue generation. In [11], an energy management system for islanded microgrids is presented that integrates different control functions. Authors in [12] and [13] approach the problem from a supervisory control theory standpoint. While these papers give a strong theoretical background towards developing supervisory controllers or schedulers, the work does not discuss the practicality of real-time implementations. Several authors have proposed machine learning based schemes that manage the execution of numerous control schemes, but the efforts are still nascent, and it is difficult to comment on the feasibility of such approaches at this stage [14], [15].

The remainder of this paper is organized as follows. In Section II, we provide an overview of well-known microgrid control functions utilized during grid-connected and grid-islanded modes of operations. In Section III, We provide the conceptual development of the scheduler and integrate the various different control functions to build the scheduler framework. Concluding remarks are presented in Section V.

II. Microgrid Control Tasks

This section describes the following microgrid control tasks: frequency control, voltage control, provision of regulation services, optimal asset dispatch, and interconnection synchronization. We start out with a description of the microgrid model adopted in this work, and then provide an overview of several control schemes that are designed to execute the aforementioned tasks. We discuss the nature of their input signals, triggering conditions, and output signals.

A. Microgrid Network Description

Consider a balanced three-phase AC microgrid whose generation units are interfaced through droop-controlled grid-forming inverters [16]–[18].[1] Suppose all loads are constant power type and all lines are short transmission lines.

For an $(n+1)$-bus microgrid, let $\mathcal{G}_p = (\mathcal{V}_p, \mathcal{E}_p)$ be an undirected simple graph representing the interconnections

[1]The setting can be easily extended to synchronous generators, grid following inverters and other grid-forming inverter technologies

between buses. The vertex or bus set, $\mathcal{V}_p$, is defined to be $\mathcal{V}_p := \{0, 1, ..., n\} = \{0\} \cup \mathcal{V}_p^{(g)} \cup \mathcal{V}_p^{(\ell)}$, and $\mathcal{V}_p^{(g)} \cap \mathcal{V}_p^{(\ell)} = \emptyset$, where bus 0 is assigned to the point of common coupling (PCC) bus, and $\mathcal{V}_p^{(g)}$ and $\mathcal{V}_p^{(\ell)}$ denote generator and load bus sets, respectively. Each bus has only a generator or load connected to it, but not both, and without loss of generality, we partition the bus set such that $\mathcal{V}_p^{(g)} := \{1, 2, ..., m\}$ and $\mathcal{V}_p^{(\ell)} := \{m+1, m+2, ..., n\}$. The edge or branch set, $\mathcal{E}_p$, is defined to be $\mathcal{E}_p \subseteq \{i, j\} : i \neq j, i, j \in \mathcal{V}_p\}$, where the edge $\{i, j\} \in \mathcal{E}_p$ if buses i and j, $i \neq j$, are connected electrically. We denote the set of buses to which each bus i is connected by $\mathcal{N}_p(i) := \{j \in \mathcal{V}_p : \{i, j\} \in \mathcal{E}_p\}$, and denote the number of such buses by $\delta_p(i) = |\mathcal{N}_p(i)|$. Let $v_i(t)$ and $\theta_i(t)$ respectively denote the magnitude and the phase of the voltage phasor associated with bus i at time t, measured relative to a reference frame that rotates at some nominal frequency. Time is discretized into fixed-time intervals, referred to as rounds, and indexed by $r = 0, 1, 2...$, and variables of interest, e.g., voltages and phase angles are indexed accordingly, e.g., $v_i[r]$ and $\theta_i[r]$ respectively denote the magnitude and phase angle of the voltage phasor at round r.

B. Secondary Frequency Control

In [3], [19], we developed and validated a secondary frequency control scheme that regulates a weighted average of the measured frequency at several buses of the microgrid to a nominal value, e.g., 60 Hz. The processor that implements this control takes as input all bus power injections and uses them to compute the so-called average frequency error, $\Delta\overline{\omega}[r]$, defined as follows

$$\Delta\overline{\omega}[r] = \frac{\sum_{i \in \mathcal{V}_p} u_i^p[r]}{\sum_{i \in \mathcal{V}_p} D_i}, \tag{1}$$

where D_i denotes the droop coefficient for each inverter-interfaced DER or load, and $u_i^p[r]$ is the active power setpoint at round r (see [3] for details). Then the DER setpoints are updated according to:

$$e_i[r+1] = e_i[r] + \kappa_i \Delta\overline{\omega}[r], \tag{2}$$

$$u_i^p[r] = u_i^{p*} + \alpha_i e_i[r], \tag{3}$$

where $e_i[0] = 0$, and α_i and κ_i are appropriately chosen gains.

C. Voltage Control

In [4], we proposed a secondary voltage control strategy that restores bus voltages to the desired range of operation. The processor that implements this control task takes as inputs voltage measurements for each bus and uses them to compute new reactive power setpoints for each DER in the microgrid. The setpoints are determined based on incremental (or decremental) DER capacity limits, and the control action is triggerred whenever a voltage magnitude violation is detected. The voltage control is implemented in two stages.

During the first stage, the reactive power setpoint at bus $i \in \mathcal{V}_p^{(g)}$, denoted by $q_i[r]$, is adjusted according to:

$$q_i[r+1] = q_i[r] + \rho[r], \tag{4}$$

$$\text{with, } \rho_i[r] = \begin{cases} \frac{\alpha}{s_{ii}}(\underline{v}_i - v_i[r]), & v_i[r] < \underline{v}_i, \\ 0, & \underline{v}_i < v_i[r] < \overline{v}_i, \\ \frac{\alpha}{s_{ii}}(\overline{v}_i - v_i[r]), & \overline{v}_i < v_i[r], \end{cases} \tag{5}$$

where $\overline{v}_i$ and $\underline{v}_i$ respectively denote upper and lower limits on the voltage magnitude at bus i, α is a constant gain and s_{ii} refers to a sensitivity factor that relates incremental changes in the voltage magnitude at bus i with incremental changes in the reactive power injection at bus i (see [4] for details).

The second stage is meant to deal with the case when there is a voltage violation at load buses or when any controllable DER fails to provide local reactive power support due to a lack of capacity. In this stage, all the controllable DERs participate together to provide the needed reactive power in the network in order to remove voltage violations. During the second stage, the reactive power setpoint at bus $i \in \mathcal{V}_p^{(g)}$ is adjusted according to:

$$q_i[r+1] = \begin{cases} \underline{q}_i, & \hat{q}_i[r+1] + \eta_i < \underline{q}_i, \\ \overline{q}_i, & \hat{q}_i[r+1] + \eta_i > \overline{q}_i, \\ \hat{q}_i[r+1] + \eta_i, & \text{otherwise}, \end{cases} \tag{6}$$

where $\hat{q}_i[r+1]$ denotes an estimate of the reactive power that is required to be injected at any bus $i \in \mathcal{V}_p^{(g)}$; details on the computation of $\eta_i,\ i \in \mathcal{V}_p^{(g)}$ are provided in [4].

D. Interchange Regulation

In [5], we implemented, and demonstrated on a C-HIL testbed, a control scheme that enables DERs within a grid-connected microgrid collectively provide frequency regulation services to the bulk grid. In this context, the Independent System Operator (ISO) sends a regulation signal, referred to as RegD in the case of PJM [5], that includes information on the desired active power interchange between the microgrid and the rest of the system, at their interconnection point(s). The processor that implements this control function takes as inputs the desired active power interchange, denoted by $\delta^p[r]$, the measured active power interchange, $u_0^p[r]$, and the active power injection of each controllable DER, $u_i^p[r],\ i \in \mathcal{V}_p^g$. Let $\Delta u_0^p[r] = \delta^p[r] - u_0^p[r]$ represent the mismatch between the desired and measured active power interchange in round r. Then, the controller updates the set-point for each DER at bus $i \in \mathcal{V}_p^{(g)}$ according to:

$$u_i^p[r+1] = u_i^p[r] + \gamma_i \Delta u_0^p[r], \tag{7}$$

where γ_i represents the participation factor for the DER at bus $i \in \mathcal{V}_p^{(g)}$. This control function is triggered whenever the microgrid is operating in grid-connected mode and there is an external command received by the controller requesting the microgrid to provide frequency regulation. We point out that the above control scheme is not just limited to provision of regulation services. In general, it can be adapted to track a desired active and reactive power interchange at the interconnection point(s) of the microgrid and the external grid.

E. Economic Dispatch

In [6], we studied the problem of optimally dispatching a collection of DERs. The problem formulation assumes that the cost associated to each DER is quadratic, and the optimal DER dispatch problem is formulated as follows:

$$\begin{aligned} \text{minimize} \quad & \sum_{i \in \mathcal{V}_p^{(g)}} \frac{(u_i^p[r] - \alpha_i)^2}{2\beta_i} \\ \text{subject to} \quad & \sum_{i \in \mathcal{V}_p^{(g)}} u_i^p[r] = D^p[r] \\ & 0 < \underline{u_i^p} \leq u_i^p[r] \leq \overline{u_i^p}, \forall i \in \mathcal{V}_p^{(g)}, \end{aligned} \tag{8}$$

where $\alpha_i \leq 0$, $\beta_i > 0$ and $D^p[r]$ is the net demand of the system in round r. The processor that implements this control task takes as input the net demand of the microgrid. The optimal dispatch problem in (8) is convex and has a separable structure (see [20]); the processor can easily find the solution by solving its Lagrange dual (see [6]) for details).

F. Interconnection Synchronization

In [7], we proposed an approach for synchronizing interconnection points of generation assets. The scheme is robust to measurement errors and load disturbances occurring during the synchronization procedure and can be leveraged to synchronize the interconnection point of a microgrid to that of another electrical power network. The synchronization scheme relies on casting the problem as an observer design problem. The idea is that by adjusting setpoints of generators in the microgrid in a specific manner, the microgrid will act as a reduced-order observer for a dynamical system whose behavior emulates the dynamics of specific bus voltage angles and frequencies that need to be (approximately) matched for successful synchronization.

III. Scheduler Development

In this section, we describe a systematic approach towards building a *scheduler* that manages the integration and execution of microgrid control schemes presented in Section II.

A. Microgrid States Description

A microgrid typically operates in *grid-connected mode* or in *islanded mode*. In each mode, multiple control functions need to be executed to ensure effective operations. In that respect, the role of the scheduler is to continuously monitor the microgrid, identify its operating mode, and appropriately execute one or more of the above control schemes so as to ensure that operational objectives are satisfied. We refer to the system that continuously monitors the microgrid as the agent. In the grid-connected mode, relevant control tasks include interchange regulation, voltage control, and economic dispatch. In the islanded mode, the microgrid has no connection to the external grid, and relevant control tasks include frequency control, voltage control, and economic dispatch. In addition, in both modes, interconnection synchronization is considered as a relevant control task for interconnecting an asset, or other microgrids, to the microgrid. Figure 1 describes the operations of the scheduler encompassing all relevant control tasks. The scheduler uses microgrid data to identify violations and schedule pertinent control schemes to correct them. The max-min consensus algorithm is used to check for convergence of the control schemes. If the convergence criteria is satisfied, then setpoints of all microgrid assets are updated accordingly. Then the process is repeated as long as the agent is online.

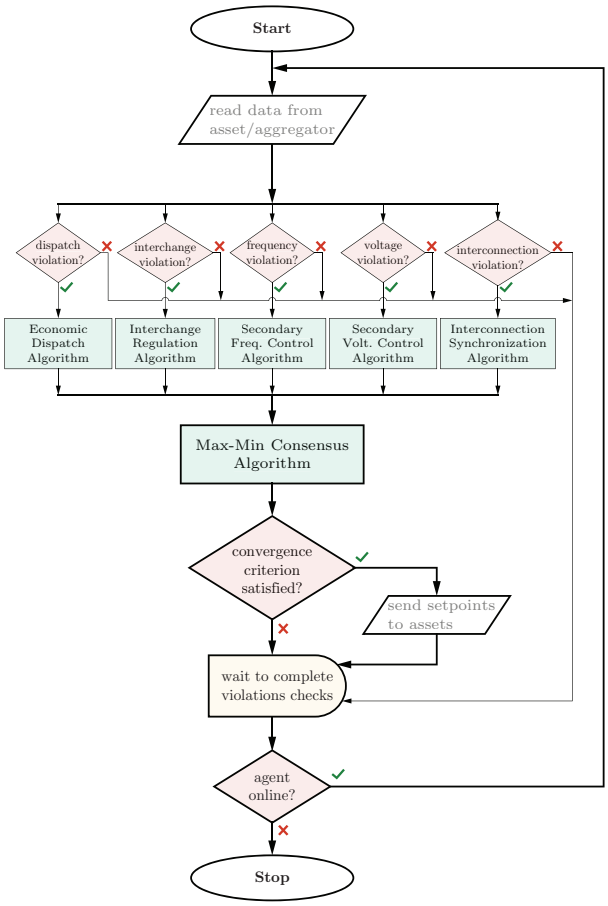

Fig. 1: Scheduler flowchart.

B. Scheduler Operations

The scheduler takes the following commands as inputs: (i) desired power interchange at the point of common coupling (PCC), i.e., the interconnection point of the microgrid and the external grid, (ii) grid connection/disconnection command, (iii) DER connection/disconnection command, and (iv) interconnection relay status. Additional inputs include bus measurements of active and reactive power injections, voltage magnitude, and frequency. Based on this information, the scheduler chooses the appropriate control task and feeds the relevant input to the individual control schemes. For example, when the interconnection relay status is ON, it means that the microgrid is in the grid-connected mode. If in addition, the ancillary service command is received, then the scheduler deploys the interchange regulation and voltage control algorithms. During this scenario, the scheduler activates the

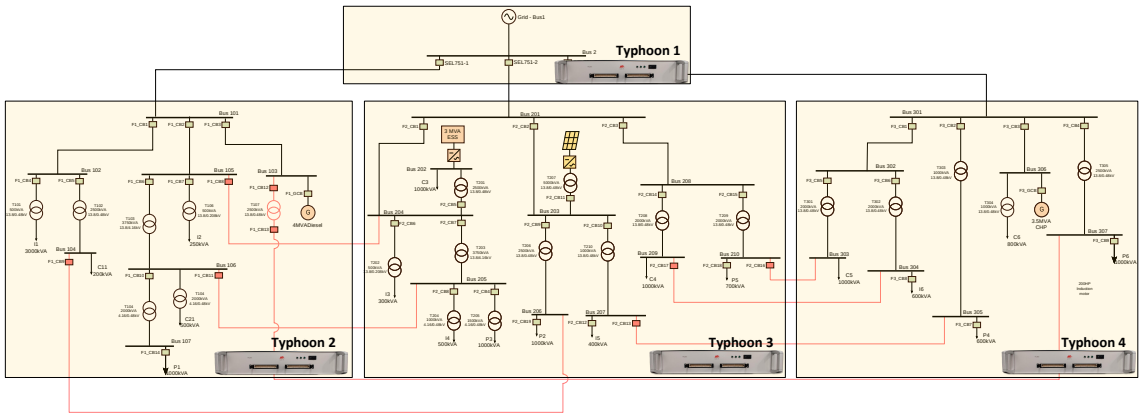

Fig. 2: Banshee distribution network emulation on Typhoon HIL 603.

economic dispatch scheme whenever the bus active power injections change by 20%, relative to the previous execution of the economic dispatch scheme. The flowchart in Fig. 1 describes operations of the control task scheduler.

IV. C-HIL Testing Results

In this section, we provide the scheduler testing results for three key operational objectives: synchronization of interconnection points between a disconnected asset and the microgrid, active power interchange regulation, and intentional islanding. A real-time emulation of the Banshee distribution network is used to verify the operations of our proposed scheduler. As depicted in Fig. 2, the Banshee system, the model of which is described in detail in [21], is emulated on four interconnected Typhoon HIL 603 devices. The distribution network comprises four DERs: two microturbines, and two DERs, one based on a grid-forming inverter, and the other based on a grid-following inverter. We point out that while the implementation of the Banshee system on our Typhoon HIL devices follows the same network configuration and resource mix as described in [21], we have implemented high-order models of each individual DER; details of the high-order modes are provided in [22].

A. Interconnection Synchronization

Here, we provide results for the synchronization of two microturbines, labeled as MT1 and MT2, to the Banshee system. Figure 3 contains two 0.03 second snapshots of the phase A voltage waveforms for the internal voltage in MT1, deployed in feeder 1, and for the bus to which it is connected during the synchronization process. As the microturbine's phase voltage, frequency and phase matches that of the bus it is interconnected to, the breaker is closed; thus, completing the synchronization of the microturbine to the network. Similarly MT2 is synchronized to feeder 3. After the synchronization process is complete, the scheduler provides an active power setpoint of 250 kW and 350 kW to MT1 and MT2 respectively. The scheduler carries out the synchronization objective in the first 65 seconds of the test. The PCC, MT1 and MT2 power injections are plotted in Fig. 4. In the entirety of the synchronization objective, the scheduler coordinates the interconnection synchronization and the voltage control schemes.

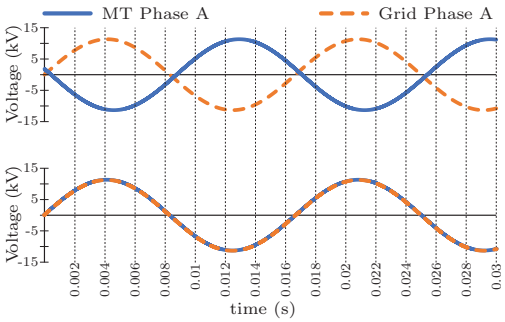

Fig. 3: Microturbine synchronization.

B. Interchange Regulation

At the 65 second mark, the scheduler receives a desired active power interchange every 10 seconds. As part of this objective, we show how the DERs increase their generation to reduce the net injection by the external grid into the Banshee system by 2 MW in the next 100 s; thus, providing frequency regulation service to the external grid. The active power injection into the Banshee system at the 65 second mark is 3200 kW and in decrements of 200 kW, the active power injection at PCC bus drops down to 1200 kW. As shown in Fig. 4, the scheduler responds to the frequency regulation command and executes the provision of frequency regulation control function to increase the generation within the microgrid in order to meet the regulation requirements. In the entirety of the provision of frequency regulation, the scheduler coordinates the frequency regulation control function and voltage control function.

C. Intentional Islanding

At 185 second mark, the scheduler receives the command to intentionally island feeder 1 and 3 of the Banshee system. As shown in Fig. 4, few seconds later, the scheduler responds to the intentional islanding command by regulating the power interchange at the PCC to zero (blue). Specifically, microturbine MT1 starts increasing its generation to take up the load of feeder 1, and microturbine MT2 starts increasing its generation to take up the load of feeder 3 as seen in

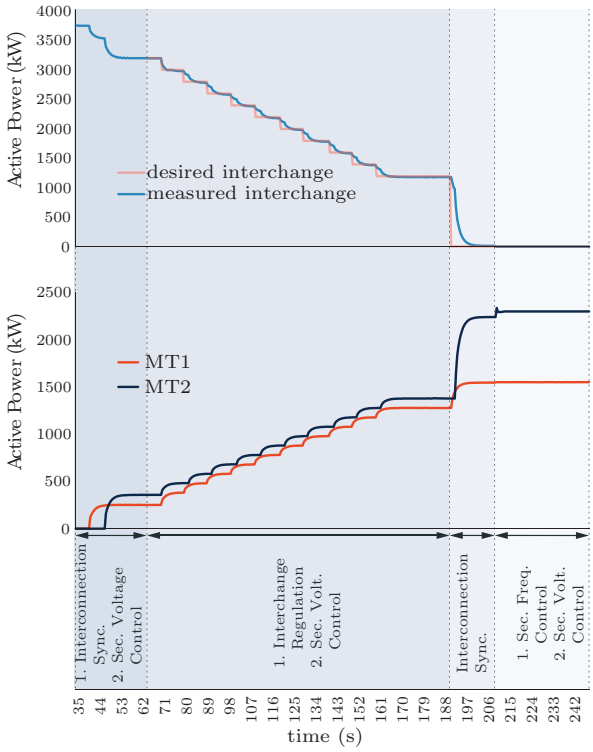

Fig. 4: PCC, microturbine (MT) 1 and 2 injections.

Fig. 4. Once the power interchange at the PCC nears zero (at 210 second mark), the scheduler sends the command to open the interconnection relay, and feeders 1 and 3 are disconnected from the external grid, as shown in Fig. 4. After the feeders have successfully islanded, the scheduler initiates execution of the control tasks associated with the islanded mode. In the entirety of the intentional islanding objective, the interchange regulation control scheme is scheduled, with the desired active and reactive power interchange set to zero. The voltage and frequency control schemes are subsequently scheduled.

V. Concluding Remarks

In this paper, we present the development and testing of a control task scheduler that manages the execution of various microgrid control schemes. We made use of the Banshee distribution network to verify and validate the scheduler under three different operational objectives i.e., new asset synchronization, active power interchange regulation, and intentional islanding.

There is scope for improvements in terms of the developed scheduler. In particular, we need to increase the capabilities of the scheduler in order for it to handle contingency scenarios such as unintentional islanding. The above work could motivate and serve as a test setup to help uncover and analyze the conflicts that can occur when multiple control schemes are not properly coordinated. Future work should explore decentralized implementations of the control task scheduler.

References

[1] North American Electric Reliability Corporation, "Distributed energy resources connection modeling and reliability considerations," Tech. Rep., 2017.

[2] D. Bakken, A. Bose, K. M. Chandy, P. P. Khargonekar, A. Kuh, S. Low, A. von Meier, K. Poolla, P. P. Varaiya, and F. Wu, "Grip - grids with intelligent periphery: Control architectures for grid2050$^{\pi}$," in *Proc. of the IEEE Smart Grid Comm.*, Oct. 2011, pp. 7–12.

[3] S. T. Cady, M. Zholbaryssov, A. D. Domínguez-García, and C. N. Hadjicostis, "A distributed frequency regulation architecture for islanded inertialess AC microgrids," *IEEE Trans. Contr. Syst. Technol.*, vol. 25, no. 6, pp. 1961–1977, Nov. 2017.

[4] B. A. Robbins, C. N. Hadjicostis, and A. D. Domínguez-García, "A two-stage distributed architecture for voltage control in power distribution systems," *IEEE Trans. Power Syst.*, vol. 28, no. 2, pp. 1470–1482, May 2013.

[5] O. Azofeifa, S. Nigam, O. Ajala, C. Sain, S. Utomi, A. D. Domínguez-García, and P. W. Sauer, "Controller hardware-in-the-loop testbed for distributed coordination and control architectures," in *Proc. of North American Power Symposium, Wichita, KS*, Oct. 2019.

[6] A. D. Domínguez-García, S. T. Cady, and C. N. Hadjicostis, "Decentralized optimal dispatch of distributed energy resources," in *Proc. of the IEEE Conference on Decision and Control*, Dec. 2012, pp. 3688–3693.

[7] O. Ajala, A. D. Domínguez-García, and D. Liberzon, "An approach to robust synchronization of electric power generators," in *Proc. of the IEEE Conference on Decision and Control*, Dec. 2018, pp. 1586–1591.

[8] R. Salcedo et al., "Banshee distribution network benchmark and prototyping platform for hardware-in-the-loop integration of microgrid and device controllers," *The Journal of Engineering*, vol. 2019, no. 8, pp. 5365–5373, 2019.

[9] G. K. Venayagamoorthy, R. K. Sharma, P. K. Gautam, and A. Ahmadi, "Dynamic energy management system for a smart microgrid," *IEEE Trans. Neural Netw. Learn Syst.*, vol. 27, no. 8, pp. 1643–1656, 2016.

[10] B. Liu, F. Zhuo, Y. Zhu, and H. Yi, "System operation and energy management of a renewable energy-based dc micro-grid for high penetration depth application," *IEEE Trans. Smart Grid*, vol. 6, no. 3, pp. 1147–1155, 2015.

[11] N. L. Díaz, A. C. Luna, J. C. Vasquez, and J. M. Guerrero, "Centralized control architecture for coordination of distributed renewable generation and energy storage in islanded AC microgrids," *IEEE Trans. Power Electron.*, vol. 32, no. 7, pp. 5202–5213, 2017.

[12] T. Dragičević, J. M. Guerrero, J. C. Vasquez, and D. Škrlec, "Supervisory control of an adaptive-droop regulated dc microgrid with battery management capability," *IEEE Trans. Power Electron.*, vol. 29, no. 2, pp. 695–706, 2014.

[13] W. H. Sadid, S. A. Abobakr, and G. Zhu, "Discrete-event systems-based power admission control of thermal appliances in smart buildings," *IEEE Trans. Smart Grid*, vol. 8, no. 6, pp. 2665–2674, 2017.

[14] G. K. Venayagamoorthy, R. K. Sharma, P. K. Gautam, and A. Ahmadi, "Dynamic energy management system for a smart microgrid," *IEEE Trans. Neural Netw. Learn Syst.*, vol. 27, no. 8, pp. 1643–1656, 2016.

[15] E. Kuznetsova, Y.-F. Li, C. Ruiz, E. Zio, G. Ault, and K. Bell, "Reinforcement learning for microgrid energy management," *Energy*, vol. 59, pp. 133–146, 2013.

[16] J. W. Simpson-Porco, F. Dörfler, and F. Bullo, "Synchronization and power sharing for droop-controlled inverters in islanded microgrids," *Automatica*, vol. 49, no. 9, pp. 2603 – 2611, 2013.

[17] M. Chandorkar, D. Divan, and R. Adapa, "Control of parallel connected inverters in standalone AC supply systems," *IEEE Trans. Ind. Appl.*, vol. 29, no. 1, pp. 136–143, 1993.

[18] K. De Brabandere, B. Bolsens, J. Van den Keybus, A. Woyte, J. Driesen, and R. Belmans, "A voltage and frequency droop control method for parallel inverters," *IEEE Trans. Power Electron.*, vol. 22, no. 4, pp. 1107–1115, 2007.

[19] S. Nigam, O. Ajala, A. D. Domínguez-García, and P. W. Sauer, "Controller hardware in the loop testing of microgrid secondary frequency control schemes," *Electr. Power Syst. Res.*, vol. 190, p. 106757, 2021.

[20] D. P. Bertsekas, "Nonlinear programming," *Journal of the Operational Research Society*, vol. 48, no. 3, pp. 334–334, 1997.

[21] E. Limpaecher, R. Salcedo, E. Corbet, S. Manson, B. Nayak, and W. Allen, "Lessons learned from hardware-in-the-loop testing of microgrid control systems," in *Proc. of the Grid of the Future Symposium Cleveland, Ohio*, Oct. 2017. [Online]. Available: https://selinc.com/

[22] O. Ajala, "A hierarchy of microgrid models with some applications," Ph.D. dissertation, University of Illinois at Urbana-Champaign, 2018.